Hindawi
Complexity
Volume 2022, Article ID 1062180, 17 pages
https://doi.org/10.1155/2022/1062180

WILEY | Hindawi

Research Article

New Variant of SARS-CoV-2 Dynamics with Imperfect Vaccine

Taye Samuel Faniran,[1] Aatif Ali,[2] Nawal E. Al-Hazmi,[3] Joshua Kiddy K. Asamoah,[4] Taher A. Nofal,[5] and Matthew O. Adewole[6]

[1]*Department of Computer Science, Lead City University, Ibadan, Nigeria*
[2]*Department of Mathematics, Abdul Wali Khan University Mardan, Khyber Pakhtunkhwa 23200, Pakistan*
[3]*Department of Chemistry, Division of Biology (Microbiology), University College of Qunfudah, Umm Al-Qura University, Qunfudah, Saudi Arabia*
[4]*Department of Mathematics, Kwame Nkrumah University of Science and Technology, Kumasi, Ghana*
[5]*Department of Mathematics and Statistics, College of Science, Taif University, P.O. Box 11099, Taif 21944, Saudi Arabia*
[6]*Department of Computer Science and Mathematics, Mountain Top University, Prayer City, Ogun State, Nigeria*

Correspondence should be addressed to Joshua Kiddy K. Asamoah; topeljoshua@gmail.com

Received 1 December 2021; Accepted 28 April 2022; Published 31 May 2022

Academic Editor: Dan Selişteanu

Copyright © 2022 Taye Samuel Faniran et al. This is an open access article distributed under the Creative Commons Attribution License, which permits unrestricted use, distribution, and reproduction in any medium, provided the original work is properly cited.

The occurrence of a new strain of SARS-CoV-2 cannot be ruled out. Therefore, this study seeks to investigate the possible effects of a hypothetical imperfect anti-COVID-19 vaccine on the control of not only the first variant of SARS-CoV-2 but also the second (new) variant of SARS-CoV-2. We further examine the rates r and a, escape of quarantined infectious individuals from isolation centers. The control R_c and basic reproduction numbers R_0 are computed which gives assess to obtain asymptotic stability of disease-free equilibrium point globally and the existence of a unique persistent equilibrium solution. Numerical results reveal that people infected with the second strain who are vaccinated with an imperfect vaccine are under control but the prevalence of the second variant enhances the prevalence of the first variant. Thus, discovering a vaccine that is effective (to a good extent) for the prevention of variant 2 (new variant) is necessary for the control of COVID-19. Numerical results also reveal that increase in the rate at which individuals infected with the first variant escape the isolation center gives rise to the population infected with the first variant and lowers the peak of the population infected with the second variant. This is probably because individuals infected with the second variant appear to be more careful with their lives and get vaccinated more than individuals infected with the first variant.

1. Introduction

Since 2019, COVID-19 has wreaked havoc in several nations, resulting in too many infections and deaths. It has resulted in several economic failures. There were also millions of confirmed COVID-19 cases and deaths worldwide. As a result of its high transmission efficiency and catastrophic infection outcomes, the disease continues to represent a hazard to human health. Coughing, sneezing, encountering sick persons, or touching things or surfaces contaminated with fecal traces are the major transmission pathways for the SARS-CoV-2 virus, according to [1]. According to [2], an imperfect vaccination is one that is unable to protect all vaccinated vulnerable persons. Vaccines must elicit an immune response similar to that elicited by a typical illness without producing the true infectious disease [3]. According to [3], there are three types of defective vaccines: the first is known as a leaky vaccine, which reduces infection but does not eliminate the risk of illness following exposure to an infectious disease. The second vaccination is an all-or-nothing vaccine that confers lifetime protection to certain individuals but does not protect others. The third vaccination, which is only effective for a limited time, is diminishing. Through transmission dynamics, many researchers have attempted to investigate and comprehend the dynamical behavior of infectious diseases [4–10].

COVID-19 articles may be found in [11–14]. In [15, 16], some optimal control problems are also established. Moshen et al. [17] also developed a mathematical model of media coverage impacts on COVID-19 dissemination. Moreover, the equilibrium solution stability requirements were discovered. Finally, they used numerical simulations to corroborate the theoretical conclusions and better understand the impact of changing factors on COVID-19 dissemination. Their findings suggest that media attention might be a useful tool for reducing illness transmission. Hattaf et al. [18] created a mathematical model to describe the dynamics of viral infections in vivo, including HIV infection. Three common incidence functions are used to represent the physical behavior of viral infection. They thoroughly studied the model basic features as well as its stability.

Hattaf et al. [18] modeled a novel within-host between SARS-CoV-2 and host pulmonary epithelial cells. Also, they developed a new generalized fractional derivative and stability [19, 20]. They included the lytic and nonlytic immune responses, as well as both mechanisms of virus-to-cell infection in the model. They proved that the model was well-posed and that equilibria existed. They looked at the model dynamical behavior using two threshold parameters. Finally, the biological implications of the analytical data were provided. A mathematical model was used by Iboi et al. [21] to estimate the influence of an imperfect anti-COVID-19 vaccination on COVID-19 control in the United States. The model theoretical analysis, as well as model fitting and parameter estimates, was completed. They used baseline parameter values acquired by fitting the model using COVID-19 mortality data for the United States to run numerical simulations of the model. Their findings revealed that an anti-COVID-19 vaccine would need to be administered to at least 82 percent of the vulnerable US population, with an estimated protective effect of 80 percent. They came to the conclusion that combining the vaccination program with other treatments such as social distance, wearing face masks, and so on will considerably improve the flawed vaccine. Olaniyi et al. [22] developed an epidemic model that took into account transmission paths from sick, asymptomatic, and hospitalized people. Using the Least Squares approach, their model was fitted to the equivalent cumulative number of hospitalized persons provided by the Nigeria Center for Disease Control (NCDC). To test the model stability around a disease-free equilibrium point, they estimated the basic reproduction number and built the Lyapunov function. They also used Pontryagin's Maximum Principle to determine the model's best control. They used numerical simulations to back up their theoretical work, and the results showed that if the disease's current effective transmission rate is decreased by 50%, the basic reproduction number in Nigeria may be reduced to less than one. Using early report case data, Nkamba and Martin Luther [23] constructed and assessed a mathematical model of the COVID-19 epidemic in Cameroon to anticipate the peak and examine the influence of containment efforts and undiagnosed sick persons on the epidemic pattern and features of COVID-19. Using appropriate Lyapunov functions, they calculated the fundamental reproduction number and established the global stability of both the disease-free and endemic equilibria. They used a sensitivity analysis to determine the most important parameters in influencing the dynamics of their model. Given the scenario in Cameroon, their findings revealed that a sluggish quarantine rate will raise the peak of infected persons, which will expand with further delays. Iboi et al. performed mathematical modeling and analysis of the COVID-19 epidemic in Nigeria [24]. They used a locally asymptotically stability analysis to provide a thorough investigation of their model. The COVID-19 Nigeria data are taken from the Nigeria Center for Disease Control (NCDC) to parameterize the model. This was used to evaluate the community-wide effect of different control and mitigation techniques over the whole Nigerian nation, as well as in two Nigerian federation states (Kano and Lagos) and the Federal Capital Territory (FCT) of Abuja. In areas where social distance, lock-down, and other community transmission reduction measures are not adopted, their findings indicated that Nigeria will have a devastatingly high COVID-19 death rate by April 2021 (in the hundreds of thousands). Parra et al. [25] developed a mathematical model of COVID-19 to investigate the effects of the emergence of a new, more transmissible SARS-CoV-2 stain in a specific location. In their model, they also included presymptomatic and asymptomatic infected people. Using the next-generation matrix approach, they were able to derive the model fundamental reproduction number, R_0. Furthermore, they proceeded the equilibria's local and global stability. Numerical simulations of the impact of a novel more infectious SARS-COV-2 strain in a population backed up their theoretical conclusions. According to their findings, a new, more infectious SARS-CoV-2 variant will arise, and the existing form prevalence will diminish.

Our work varies from previous COVID-19 research in the following ways. Anggriani et al. [11] developed and assessed a COVID-19 mathematical model that included the transmission path of asymptomatic and symptomatic compartments, as well as decreasing immunity, without taking into account the effect of vaccination on the novel SARS-CoV-2 variant. To guarantee that COVID-19 vaccinations give maximum protection in the future, researchers must investigate the influence of an incomplete anti-COVID-19 vaccine on the new variation. To analyze and monitor the COVID-19 epidemic, Youssef et al. [26] suggested a modified version of the Susceptible-Exposed-Infectious-Quarantined-Recovered (SEIQR) essential disease dynamics model for the COVID-19 emergence. They only examined the standard Susceptible-Exposed-Infectious-Quarantined-Recovered of COVID-19, ignoring the possibility of a new SARS-CoV-2 variation and the impact of the present anti-COVID-19 vaccination on the new variety. Parra et al. [25] proposed an ordinary differential equation-based model to investigate a new more transmissible SARS-CoV-2 strain through the transmission route of exposed, presymptomatic, symptomatic, and asymptomatic classes, but they did not look into the impact of the COVID-19 vaccine on the new more transmissible SARS-CoV-2 strain. The absence of vaccinated persons in the presence of the new strain is costly since it is necessary to determine if the current

COVID-19 vaccination protects against the new strain. As a result, the current study will fill in all of the gaps mentioned above.

SARS-CoV-2 has recently been discovered in various countries with a novel strain that offers a greater hazard to humans. The current study investigates the impact of an imperfect vaccine on the dynamics of COVID-19 with two SARS-CoV-2 variants, which was inspired by a paper [25], in which they proposed two SARS-CoV-2 variants and pre-symptomatic infectious individuals on the dynamics of COVID-19. This distinguishes our work from that of [25]. The unique component of this work is modeling a new version of SARS-CoV-2 transmission dynamics in order to analyze the influence of a hypothetical imperfect anti-COVID-19 vaccination on the control of both the first and second variants of SARS-CoV-2. It is critical and necessary to determine how well the current antigen-specific COVID-19 vaccine protects individuals against the new variant so that scientists can determine whether an update to the current antigen-specific anti-COVID-19 vaccine is required to ensure that the COVID-19 vaccine continues to provide optimal protection as new antigenically distinct variants emerge in the future. Furthermore, we include the influence of the escape rate of quarantined infected persons from isolation facilities in Nigeria in our model owing to fears or beliefs that the government is utilizing the epidemic to enrich its pockets in Nigeria [27]. None of the most current and most recent publications on COVID-19, such as [11, 25, 26, 28–30], have taken these specific elements into account. Individuals should be aware that the COVID-19 vaccine does not provide 100 percent protection since immunization is one of the most effective advancements in disease prevention. On the other hand, it is crucial that everyone (with the exception of individuals with severe allergy diseases) obtains a vaccine. As a result, we develop a mathematical model that accounts for poor vaccination on both SARS-CoV-2 types. To support the analytical conclusions, a global study of the model is performed and numerical simulations are shown.

The research aims and importance of the study are highlighted in the following sections based on the above.

1.1. Objectives.

(1) To explore the impact of the new variant of SARS-CoV-2 in a population, in the presence of an imperfect vaccine

(2) To examine the behavior of solution trajectories of the model when the new variant transmission rate of SARS-CoV-2 is higher than the pre-existing one [31]

(3) To determine the impact of escape of quarantined infectious individuals from isolation centers

1.2. Significance.

(1) The study will help the health authorities to know the significance of imperfect vaccination on the transmission dynamics in the presence of a new variant of SARS-CoV-2.

(2) The study will help to know whether vaccinating the population against the new variant of SARS-CoV-2 plays a role in the control reproduction number.

(3) The evaluation of analytical results will provide useful information that will help to eradicate COVID-19 in the population.

(4) The study will help the policymakers on health to have a clear picture of the impact of imperfect vaccination against the new variant.

(5) The research will aid government officials in recognizing the risk of COVID-19 patients fleeing isolation facilities and developing strategies to educate them in their different local languages and dialects about COVID-19 and the repercussions of refusing the government free treatment.

2. Mathematical Formulation of COVID-19 Model

This section describes the transmission dynamics of COVID-19, and the formulated model is presented, respectively. The total individual population, denoted by N, is divided into nine categories: susceptible individuals S, vaccinated individuals V (individuals who get vaccinated), two classes of exposed individuals $E_{1,2}$, two classes of quarantined infectious individuals $Q_{1,2}$, two classes of unquarantined infectious individuals $U_{1,2}$, and recovered individuals R, so that $N = S + V + E_1 + E_2 + Q_1 + Q_2 + U_1 + U_2 + R$.

The susceptible individuals population is generated by the recruitment of individuals into the population, either by birth or immigration, at the rate Λ. We assume that individuals would belong to one of the classes described above, depending on the COVID-19 status [25]. We also assume that vaccine is not perfect, and therefore vaccinated individuals may contact the virus at the rates $\alpha(1-\psi_1)$ and $\eta(1-\psi_2)$, where $\psi_1 \in [0,1]$ and $\psi_2 \in [0,1]$ represent the vaccine efficacy against variant 1 and variant 2. Furthermore, it is noteworthy that $\psi_1 = 1$ and $\psi_2 = 1$ imply that a vaccine provides 100% assurance against COVID-19, while $\psi_1 = 0$ and $\psi_2 = 0$ indicate a vaccine that does not secure individuals in any way. Furthermore, because the vaccine was designed to protect against variant 1, we assume that its efficacy against variant 2 is less than its efficacy against variant 1 (i.e., $\psi_2 < \psi_1$). It is also assumed that someone who is infected with the first variant of SARS-CoV-2 cannot catch the second variant (the new variant) due to an acquired immune response [32, 33]. There is a progression rate from quarantined infectious individual compartments to unquarantined infectious individual compartments due to the probability of fleeing isolation centers. It is assumed that quarantined infectious individuals are not severely sick (i.e., they are moderately or mildly sick). By assumption, there is no loss of immunity [25].

Applying the biological assumptions, nomenclature of parameters in Table 1, the following system is formulated:

$$\begin{cases} \dfrac{dS}{dt} = \Lambda - \alpha S U_1 - \eta S U_2 - (\kappa + \mu) S, \\ \dfrac{dV}{dt} = \kappa S - \alpha(1-\psi_1) V U_1 - \eta(1-\psi_2) V U_2 - \mu V, \\ \dfrac{dE_1}{dt} = \alpha S U_1 + \alpha(1-\psi_1) V U_1 - (\beta + \mu) E_1, \\ \dfrac{dQ_1}{dt} = (1-\theta)\beta E_1 - (r + \tau_1 + \mu + \delta_1) Q_1, \\ \dfrac{dU_1}{dt} = \theta\beta E_1 + r Q_1 - (\tau_2 + \delta_2 + \mu) U_1, \\ \dfrac{dE_2}{dt} = \eta S U_2 + \eta(1-\psi_2) V U_2 - (p + \mu) E_2, \\ \dfrac{dQ_2}{dt} = (1-b) p E_2 - (a + c_1 + \mu + \delta_3) Q_2, \\ \dfrac{dU_2}{dt} = b p E_2 + a Q_2 - (c_2 + \mu + \delta_4) U_2, \\ \dfrac{dR}{dt} = \tau_1 Q_1 + \tau_2 U_1 + c_1 Q_2 + c_2 U_2 - \mu R, \end{cases} \tag{1}$$

with initial conditions such as

$$\begin{aligned} S(0) &= S_0 > 0, \\ V(0) &= V_0 > 0, \\ E_1(0) &= E_{1_0} > 0, \\ Q_1(0) &= Q_{1_0} > 0, \\ U_1(0) &= U_{1_0} > 0, \\ E_2(0) &= E_{2_0} > 0, \\ Q_2(0) &= Q_{2_0} > 0, \\ U_2(0) &= U_{2_0} > 0, \\ R(0) &= R_0 > 0, \end{aligned} \tag{2}$$

where the model parameters are nonnegative. For biological reasons, the model is analyzed in the feasible-region as follows:

$$D = \left((S, V, E_1, Q_1, U_1, E_2, Q_2, U_2, R) \in \Re_+^9 : 0 \le S \le \frac{\Lambda}{\mu + \kappa}, 0 \le V \le \frac{\kappa \Lambda}{\mu(\mu + \kappa)}, N \le \frac{\Lambda}{\mu} \right), \tag{3}$$

that shows system (1) is to be positively invariant. Thus, the model is well-posed both mathematically and epidemiologically in D. The first eight equations of system (1) do not affect the compartments R, and therefore we have

$$\begin{cases} \dfrac{dS}{dt} = \Lambda - \alpha S U_1 - \eta S U_2 - (\kappa + \mu) S, \\ \dfrac{dV}{dt} = \kappa S - \alpha(1-\psi_1) V U_1 - \eta(1-\psi_2) V U_2 - \mu V, \\ \dfrac{dE_1}{dt} = \alpha S U_1 + \alpha(1-\psi_1) V U_1 - (\beta + \mu) E_1, \\ \dfrac{dQ_1}{dt} = (1-\theta)\beta E_1 - (r + \tau_1 + \mu + \delta_1) Q_1, \\ \dfrac{dU_1}{dt} = \theta\beta E_1 + r Q_1 - (\tau_2 + \delta_2 + \mu) U_1, \\ \dfrac{dE_2}{dt} = \eta S U_2 + \eta(1-\psi_2) V U_2 - (p + \mu) E_2, \\ \dfrac{dQ_2}{dt} = (1-b) p E_2 - (a + c_1 + \mu + \delta_3) Q_2, \\ \dfrac{dU_2}{dt} = b p E_2 + a Q_2 - (c_2 + \mu + \delta_4) U_2. \end{cases} \tag{4}$$

Table 1: Summary of the parameters.

Parameter	Meaning	Value	Reference
N_0	Initial population size	500,000	Assumed
α	Contact rate between S and U_1	$0.5/N_0\text{day}^{-1}$	[24]
η	Contact rate between S and U_2	$0.65/N_0\text{day}^{-1}$	[24]
θ	Fraction of E_1 who are unquarantined infectious	0.3	Assumed
b	Fraction of E_2 who are unquarantined infectious	0.3	Assumed
τ_1	Recovery rate of quarantined infectious individuals	0.0815day^{-1}	[34]
τ_2	Recovery rate of unquarantined infectious individuals	$1/14\text{day}^{-1}$	[35]
c_1	Recovery rate of Q_2	0.0815day^{-1}	[34]
c_2	Recovery rate of U_2	$1/14\text{day}^{-1}$	[35]
r	Probability of fleeing isolation centers of Q_1	0.01day^{-1}	Assumed
a	Probability of fleeing isolation centers of Q_2	0.01day^{-1}	Assumed
κ	Vaccination rate	$1/42\text{day}^{-1}$	Assumed
Λ	Recruitment rate	$N_0\mu\text{day}^{-1}$	Assumed
μ	Natural death rate	0.01186year^{-1}	[36, 37]
β	Incubation rate of SARS-CoV-2	$0.142\ \text{day}^{-1}$	[23]
p	Incubation rate of new variant of SARS-CoV-2	$0.0152\ \text{day}^{-1}$	Assumed
δ_1	Disease-induced death rate of Q_1	0.015	[24]
δ_2	Disease-induced death rate of U_1	0.015	[24]
δ_3	Disease-induced death rate of Q_2	0.02day^{-1}	Assumed
δ_4	Disease-induced death rate of U_2	0.02day^{-1}	Assumed
ψ_1	Vaccine efficacy against variant 1	[0.1 – 0.7]	Assumed
ψ_2	Vaccine efficacy against variant 2	[0.1 – 0.65]	Assumed

2.1. Basic Reproduction Number. To determine the overall dynamical behavior of the equilibrium solution, the control reproduction number, R_c, will be used. R_c is computed as the difference between the rate of new infection in each infected compartment F and the rate of transfer between each infected compartment G using the approach [38]. As a result, we have

$$\begin{pmatrix} \frac{dE_1}{dt} \\ \frac{dQ_1}{dt} \\ \frac{dU_1}{dt} \\ \frac{dE_2}{dt} \\ \frac{dQ_2}{dt} \\ \frac{dU_2}{dt} \end{pmatrix} = F - G = \begin{pmatrix} \alpha S U_1 + \alpha(1-\psi)_1 V U_1 \\ 0 \\ 0 \\ \eta S U_2 + \eta(1-\psi_2) V U_2 \\ 0 \\ 0 \end{pmatrix} - \begin{pmatrix} (\beta+\mu)E_1 \\ -(1-\theta)\beta E_1 + (r+m_1)Q_1 \\ -\theta\beta E_1 - rQ_1 + m_2 U_1 \\ (p+\mu)E_2 \\ -(1-b)pE_2 + (a+m_3)Q_2 \\ -bpE_2 - aQ_2 + m_4 U_2 \end{pmatrix}, \tag{5}$$

where

$$\begin{aligned} m_1 &= \tau_1 + \mu + \delta_1, \\ m_2 &= \tau_2 + \mu + \delta_2, \\ m_3 &= c_1 + \mu + \delta_3, \\ m_4 &= c_2 + \mu + \delta_4. \end{aligned} \tag{6}$$

The disease-free equilibrium is

$$\begin{aligned} W^0 &= \left(S^0, V^0, E_1^0, Q_1^0, U_1^0, E_2^0, Q_2^0, U_2^0\right) \\ &= \left(\frac{\Lambda}{\mu+\kappa}, \frac{\kappa\Lambda}{\mu(\mu+\kappa)}, 0, 0, 0, 0, 0, 0\right). \end{aligned} \tag{7}$$

Consequently, R_c for the first and second variants is given as

$$R_c = \max\left\{R_{FV_c}, R_{SV_c}\right\}, \tag{8}$$

where

$$R_{FV_c} = \frac{\Lambda\beta\alpha(\theta m_1 + r)(\mu + (1-\psi_1)\kappa)}{m_2\mu(\beta+\mu)(m_1+r)(\kappa+\mu)}, \tag{9}$$

and

$$R_{SV_c} = \frac{\Lambda p\eta(bm_3 + a)(\mu + (1-\psi_2)\kappa)}{m_4\mu(p+\mu)(m_3+a)(\kappa+\mu)}. \tag{10}$$

Rc is used as an invasion threshold for both predicting COVID-19 outbreaks and assessing control strategies that would reduce COVID-19 spread in the community by lowering *Rc* and parameters that would increase disease spread by increasing *Rc*. When control methods are ineffectual, the value of R_0 may be calculated from the value of R_c, in the sense that $\psi_1 = 0$, $\psi_2 = 0$, and $\kappa = 0$. As a result, without any control mechanisms, the basic reproduction number is

$$R_0 = \max\{R_{FV}, R_{SV}\}, \tag{11}$$

where

$$R_{FV} = \frac{\Lambda\beta\alpha(\theta m_1 + r)}{m_2\mu(\beta+\mu)(m_1+r)}, \tag{12}$$

and

$$R_{SV} = \frac{\Lambda p\eta(bm_4 + a)}{m_5\mu(p+\mu)(m_4+a)}. \tag{13}$$

However, our analysis will be based on the control reproduction number, R_c. Furthermore, it is assumed that the population is completely susceptible initially, and R_c measures the average secondary cases at the beginning of the epidemic.

3. Stability Analysis

The global asymptotic stability for the disease-free equilibrium is examined by following a positive definite Lyapunov function. See [22, 23, 39] for further information on the creation of the Lyapunov function.

3.1. Global Stability of Disease-Free Equilibrium

Theorem 1. *The disease-free equilibrium is globally asymptotically stable if* $R_c < 1$.

Proof. Consider the Lyapunov function as follows:

$$L = \beta(\theta m_1 + r)E_1 + r(\beta+\mu)Q_1 + (\beta+\mu)(m_1+r)U_1 + p(bm_3+a)E_2 + a(p+\mu)Q_2 + (p+\mu)(m_3+a)U_2. \tag{14}$$

The time derivative of (10) along the COVID-19 model (4) is

$$\begin{aligned}
\dot{L} &= \beta(\theta m_1 + r)(\alpha S U_1 + \alpha(1-\psi_1)VU_1 - (\beta+\mu)E_1) + r(\beta+\mu)((1-\theta)\beta E_1 - (m_1+r)Q_1)\\
&\quad + (\beta+\mu)(m_1+r)(\theta\beta E_1 + rQ_1 - m_2U_1) + p(bm_3+a)(\eta S U_2 + \eta(1-\psi_2)VU_2 - (p+\mu)E_2)\\
&\quad + a(p+\mu)((1-b)pE_2 - (a+m_3)Q_2) + (p+\mu)(m_3+a)(bpE_2 + aQ_2 - m_4U_2),\\
&= \beta(\theta m_1 + r)\alpha S U_1 + \alpha(1-\psi_1)VU_1 - \beta(\theta m_1 + r)(\beta + \mu E_1) + r(\beta+\mu)\beta E_1\\
&\quad - r(\beta+\mu)\theta\beta E_1 - (\beta+\mu)(m_1+r)m_2U_1 + p(bm_3+a)\eta S U_2 + \eta(1-\psi_2)VU_2 - p(bm_4+a)(p+\mu E_2)\\
&\quad + a(p+\mu)pE_2 - a(p+\mu)bpE_2 - (p+\mu)(m_3+a)m_4U_2,\\
&= \beta(\theta m_1 + r)\alpha S U_1 + \alpha(1-\psi_1)VU_1 - \beta(\theta m_1 + r)(\beta+\mu)E_1 + r(\beta+\mu)(1-\theta)\beta E_1 + (\beta+\mu)(m_1+r)\theta\beta E_1\\
&\quad - (\beta+\mu)(m_1+r)m_2U_1 + p(bm_3+a)\eta S U_2 + \eta(1-\psi_2)VU_2\\
&\quad - p(bm_3+a)(p+\mu)E_2 + a(p+\mu)(1-b)pE_2 + (p+\mu)(m_4+a)bpE_2 - (p+\mu)(m_3+a)m_4U_2,\\
&= \beta(\theta m_1 + r)\alpha S U_1 + \alpha(1-\psi_1)VU_1 - r\beta E_1(\beta+\mu)(1-\theta) + r(\beta+\mu)(1-\theta)\beta E_1\\
&\quad - (\beta+\mu)(m_1+r)m_2U_1 + p(bm_3+a) + \eta S U_2 + \eta(1-\psi_2)VU_2 - apE_2(p+\mu)(1-b)\\
&\quad + a(p+\mu)(1-b)pE_2 - (p+\mu)(m_3+a)m_4U_2,\\
&= (\beta+\mu)(m_1+r)m_2U_1\left(\frac{\Lambda\beta\alpha(\theta m_1+r)\mu + (1-\psi_1)\kappa}{m_2\mu(\beta+\mu)(m_1+r)(\kappa+\mu)} - 1\right) + (p+\mu)(m_3+a)m_4U_2\left(\frac{\Lambda p\eta(bm_3+a)\mu + (1-\psi_2)\kappa}{m_4\mu(p+\mu)(m_3+a)(\kappa+\mu)} - 1\right),\\
&= m_2(\beta+\mu)(m_1+r)\left(R_{FV_c} - 1\right)U_1 + m_5(\rho+\mu)(m_3+a)\left(R_{SV_c} - 1\right)U_2, \leq (m_2(\beta+\mu)(m_1+r)U_1 + m_4(\rho+\mu)(m_3+a)U_2)(R_c - 1).
\end{aligned} \tag{15}$$

Furthermore, $\dot{L} = 0 \leftrightarrow Q_1 = 0, U_1 = 0$ and $Q_2 = 0, U_2 = 0$ or $S = S^0$, $V = V^0$, and $R_c = 1$.

Thus, the singleton set is the biggest compact invariant set in $(S, ; V, ; E_1, ; Q_1, ; U_1, ; E_2, ; Q_2, ; U_2) \in D : \dot{L} = 0$, and $W0$ is globally asymptotically stable in D according to LaSalle's Invariance Principle [40]. The aforementioned result has the epidemiological implication that the starting sizes of the model's subpopulation (i.e., the initial number of sick persons) introduced into the community do not have to be within the model's disease-free equilibrium W^0 base of attraction. For $R_c < 1$, this suggests that COVID-19 can be eradicated regardless of the original size of the infectious population. □

3.2. Existence and Uniqueness of Endemic Equilibrium Solution. We will show that the formulated COVID-19 model contains an endemic equilibrium point, W_1. The COVID-19 infection continues in the population at the endemic equilibrium point, which is a positive steady-state solution. The solution trajectories of the model are analyzed; when the transmission routes of the second variant of SARS-CoV-2 are higher than the first variant [25], we establish the existence of a single endemic equilibrium point if the condition $\eta U_2^* > \alpha U_1^*$ and then $E_1^* = U_1^* = 0$ hold. The impact of the second SARS-CoV-2 variant on the dynamics of COVID-19 in light of defective vaccination in particular countries at the time of advance is determined analytically. The following are the equations:

$$\begin{cases} \Lambda - \alpha S^* U_1^* - \eta S^* U_2^* - (\kappa + \mu) S^* = 0, \\ \kappa S^* - \alpha(1-\psi_1) V^* U_1^* - \eta(1-\psi_2) V^* U_2^* - \mu V^* = 0, \\ (1-b) p E_2^* - (a + c_1 + \mu + \delta_3) Q_2^* = 0, \\ b p E_2^* + a Q_2^* - (c_2 + \mu + \delta_4) U_2^* = 0. \end{cases} \tag{16}$$

Let $W_1 = (S^*, V^*, E_2^*, Q_2^*)$ where S^*, V^*, E_2^*, and Q_2^* can be found from (16) to be

$$\begin{cases} S^* = \dfrac{\Lambda}{\alpha U_1^* + \eta U_2^* + \kappa + \mu}, \\ V^* = \dfrac{\Lambda \kappa}{(\alpha U_1^* + \eta U_2^* + \kappa + \mu)(\alpha(1-\psi_1) U_1^* + \eta(1-\psi_2) U_2^* + \mu)}, \\ E_2^* = \dfrac{(a + m_3) Q_2^*}{(1-b) p}, \\ Q_2^* = \dfrac{m_4 (1-b) p (m_3 + a)}{(m_3 + a) p (a + b m_3)} U_2^*. \end{cases} \tag{17}$$

The following equations for U_1^* and U_2^* are obtained after substituting (16) into (17),

$$\frac{\eta \Lambda (\alpha(1-\psi_1) U_1^* + \eta(1-\psi_2) U_2^* + \mu + \kappa(1-\psi_2))}{(\alpha U_1^* + \eta U_2^* + \kappa + \mu)(\alpha(1-\psi_1) U_1^* + \eta(1-\psi_2) U_2^* + \mu)} - \frac{(p+\mu) m_4 (a + m_3)}{p(b m_3 + a)} = 0. \tag{18}$$

If we let

$$f(x_1, x_2) = \frac{\eta \Lambda (\alpha(1-\psi_1) x_1 + \eta(1-\psi_2) x_2 + \mu + \kappa(1-\psi_2))}{(\alpha x_1 + \eta x_2 + \kappa + \mu)(\alpha(1-\psi_1) x_1 + \eta(1-\psi_2) x_2 + \mu)} - \frac{(p+\mu) m_4 (a + m_3)}{p(b m_3 + a)}, \tag{19}$$

so that $\dot{f}(x_1, x_2) < 0$, $\lim_{a \longrightarrow +\infty}$, $f(x_1, x_2) < 0$, and

$$f(0) = \frac{(m_4 (p+\mu)(m_3 + a))}{p(a + b m_3)} \left(R_{SV_c} - 1\right). \tag{20}$$

In the sense that if $R_{SV_c} > 1$, then $f(0) > 0$. Thus, for the equation $f(a) = 0$, a unique positive solution exists only when $R_{SV_c} > 1$.

Theorem 2. *Model (4) has a unique W_1 whenever $R_{SV_c} > \max\{R_{FV_c,1}\}$.*

3.3. Global Stability of Endemic Equilibrium Solution (W_1). In order to show that COVID-19 in the population persists and converges to W_1, the following result is stated and proved.

Theorem 3. *The unique equilibrium W_1 is globally asymptotically stable (GAS) whenever $R_c > 1$.*

Proof. Given the following equations at the endemic equilibrium point W_1:

$$\begin{cases} \Lambda = \mu S^* + \mu V^* + \alpha S^* U_1^* + \eta S^* U_2^* + \alpha U_1^* (1-\psi_1) V^* + \eta U_2^* (1-\psi_2) V^*, \\ \kappa S^* = \alpha (1-\psi_1) V^* U_1^* + \eta (1-\psi_2) V^* U_2^* + \mu V^*, \\ (\beta + \mu) E_1^* = \alpha S^* U_1^* + \alpha (1-\psi_1) V^* U_1^*, \\ (p+\mu) E_2^* = \eta S^* U_2^* + \eta (1-\psi_2) V^* U_2^*, \\ Q_1^* = \dfrac{(1-\theta)\mu U_1^*}{\theta\mu + r}, \\ Q_2^* = \dfrac{(1-b)\mu U_2^*}{b\mu + a}. \end{cases} \tag{21}$$

Let

$$X = \left(S^*, V^*, E_1^*, E_2^*, Q_1^*, Q_2^*, U_1^*, U_2^*\right)^T \in \Re_+^8. \tag{22}$$

And consider the following Lyapunov function:

$$\begin{aligned} V(x) = {} & \left(S - S^* - S^* \ln \frac{S}{S^*}\right) + \left(V - V^* - V^* \ln \frac{V}{V^*}\right) + \left(E_1 - E_1^* - E_1^* \ln \frac{E_1}{E_1^*}\right) + d_1 \left(Q_1 - Q_1^* - Q_1^* \ln \frac{Q_1}{Q_1^*}\right) \\ & + d_2 \left(Q_2 - Q_2^* - Q_2^* \ln \frac{Q_2}{Q_2^*}\right) + f_1 \left(U_1 - U_1^* - U_1^* \ln \frac{U_1}{U_1^*}\right) + f_2 \left(U_2 - U_2^* - U_2^* \ln \frac{U_2}{U_2^*}\right), \end{aligned} \tag{23}$$

where

$$\begin{aligned} d_1 &= \frac{\alpha r \left(S^* + (1-\psi_1) V^*\right)}{\mu(\mu + r)}, \\ d_2 &= \frac{\eta a \left(S^* + (1-\psi_2) V^*\right)}{\mu}, \\ f_1 &= \frac{\alpha \left(S^* + (1-\psi_1) V^*\right)}{\mu}, \\ f_2 &= \frac{\eta \left(S^* + (1-\psi_2) V^*\right)}{\mu}. \end{aligned} \tag{24}$$

Differentiating V with respect to time gives

$$\begin{aligned} \dot{V}(x) = {} & \left(1 - \frac{S^*}{S}\right)\dot{S} + \left(1 - \frac{V^*}{V}\right)\dot{V} + \left(1 - \frac{E_1^*}{E_1}\right)\dot{E}_1 + \left(1 - \frac{E_2^*}{E_2}\right)\dot{E}_2 + d_1 \left(1 - \frac{Q_1^*}{Q_1}\right)\dot{Q}_1 + d_2 \left(1 - \frac{Q_2^*}{Q_2}\right)\dot{Q}_2 \\ & + f_1 \left(1 - \frac{U_1^*}{U_1}\right)\dot{U}_1 + f_2 \left(1 - \frac{U_2^*}{U_2}\right)\dot{U}_2. \end{aligned}$$

$$\begin{aligned}\dot{V}(x) = &\left(1-\frac{S^*}{S}\right)(\Lambda-\alpha SU_1-\eta SU_2-(\kappa+\mu)S)+\left(1-\frac{V^*}{V}\right)(\kappa S-\alpha(1-\psi_1)VU_1-\eta(1-\psi_2)VU_2-\mu V)\\&+\left(1-\frac{E_1^*}{E_1}\right)(\alpha SU_1+\alpha(1-\psi_1)VU_1-(\beta+\mu)E_1)+\left(1-\frac{E_2^*}{E_2}\right)(\eta SU_2+\eta(1-\psi_2)VU_2-(p+\mu)E_2)\\&+d_1\left(1-\frac{Q_1^*}{Q_1}\right)((1-\theta)\beta E_1-(r+m_1)Q_1)+d_2\left(1-\frac{Q_2^*}{Q_2}\right)((1-b)pE_2-(a+m_3)Q_2)\\&+f_1\left(1-\frac{U_1^*}{U_1}\right)(\theta\beta E_1+rQ_1-m_2U_1)+f_2\left(1-\frac{U_2^*}{U_2}\right)(bpE_2+aQ_2-m_4U_2).\end{aligned}\tag{25}$$

After developing and using (21), we have the following:

$$\begin{aligned}\dot{V}(x) = &\frac{-\mu}{S}(S-S^*)^2+\alpha U_1^*(S^*+(1-\psi_1)V^*)+\eta U_2^*(S^*+(1-\psi_2)V^*)+\kappa S^*+\mu V^*-\mu V-\kappa S\frac{V^*}{V}\\&+d_1((1-\theta)\beta+f_1\theta\beta E_1-\mu-\beta)E_1+d_2((1-b)p+f_2bpE_2-\mu-p)E_2-\alpha SU_1\frac{E_1^*}{E_1}\\&-(1-\psi_1)\alpha VU_1\frac{E_1^*}{E_1}-(1-\psi_2)\eta VU_2\frac{E_2^*}{E_2}+(\mu+\beta)E_1^*-(p+\mu)E_2^*+(f_1r-d_1(\mu+r))Q_1\\&+(f_2a-d_2(\mu+a))Q_2-d_1(1-\theta)\beta E_1\frac{Q_1^*}{Q_1}-d_2(1-b)pE_2\frac{Q_2^*}{Q_2}+d_1(\mu+r)Q_1^*+d_2(\mu+a)Q_2^*\\&+(-f_1\mu+\alpha U_1^*+(1-\psi_1)\alpha V^*)U_1+(-f_2\mu+\eta U_2^*+(1-\psi_2)\eta V^*)U_2-f_1\theta\beta E_1\frac{U_1^*}{U_1}-f_2pbE_2\frac{U^*}{U_2}\\&-f_1rQ_1\frac{U_1^*}{U_1}-f_2aQ_2\frac{U_2^*}{U_2}+f_1\mu U_1^*+f_2\mu U_2^*.\end{aligned}\tag{26}$$

Substituting d_1, d_2, f_1, and f_2 by their values and exploiting, we have

$$\begin{aligned}\dot{V}(x) = &\frac{-\mu}{S}(S-S^*)^2+\mu V^*\left(3-\frac{S^*}{S}-\frac{V}{V^*}-\frac{SV^*}{S^*V}\right)+\alpha U_1^*S^*\left(3+\frac{r(1-\theta)}{\theta\mu+r}\right)+\eta U_2^*S^*\left(3+\frac{a(1-b)}{b\mu+a}\right)\\&+(1-\psi_1)\alpha U_1^*V^*\left(4+\frac{r(1-\theta)}{\theta\mu+r}\right)+(1-\psi_2)\eta U_2^*V^*\left(4+\frac{a(1-b)}{b\mu+a}\right)-\eta SU_2\frac{E_2^*}{E_2}-\alpha SU_1\frac{E_1^*}{E_1}\\&-(1-\psi_1)\alpha VU_1\frac{E_1^*}{E_1}-(1-\psi_2)\eta VU_2\frac{E_2^*}{E_2}-\frac{(1-\psi_1)\alpha SU_1^*V^{*2}}{S^*V^*}-\frac{(1-\psi_2)\eta SU_2^*V^{*2}}{S^*V^*}\\&-\frac{\alpha r(1-\theta)(S^*+(1-\psi_1)V^*)U_1^*}{(\theta\mu+r)}-\frac{\eta a(1-b)(S^*+(1-\psi_2)V^*)U_2^*}{(b\mu+a)}-\frac{\eta a(S^*+(1-\psi_2)V^*)Q_2U_2^*}{\mu U_2}\\&-\frac{\alpha\theta\beta(S^*+(1-\psi_1)V^*)E_1U_1^*}{\mu U_1}-\frac{\eta bp(S^*+(1-\psi_2)V^*)E_2U_2^*}{\mu U_2}-\frac{\alpha r(S^*+(1-\psi_1)V^*)Q_1U_1^*}{\mu U_1}.\end{aligned}\tag{27}$$

Define

$$g = \frac{(1-\theta)r}{\theta\mu + r},$$
$$k = \frac{\theta(\mu + r)}{\theta\mu + r},$$
$$h = \frac{(1-b)a}{b\mu + a}, \tag{28}$$
$$s = \frac{b(\mu + a)}{b\mu + a}.$$

Then,

$$\begin{aligned} &g + h = 1, k + s = 1,\\ &3 + g = 3g + 3k + g, = 3k + 4g,\\ &3 + h = 3h + 3s + h, = 3s + 4h,\\ &4 + g = 4k + 5g4 + h = 4s + 5h. \end{aligned} \tag{29}$$

$\dot{V}(x)$ can be rewritten as

$$\begin{aligned} \dot{V}(x) = {} & \frac{-\mu}{S}(S - S^*)^2 + \mu V^*\left(3 - \frac{S^*}{S} - \frac{V}{V^*} - \frac{SV^*}{S^*V}\right) + (3h + 4g)\alpha S^*U_1^* + (3s + 4k)\eta S^*U_2^*\\ & + (4h + 5g)(1 - \psi_1)\alpha V^*U_1^* + (4s + 5k)(1 - \psi_2)\eta V^*U_2^* - \alpha SU_1\frac{E_1^*}{E_1} - \eta SU_2\frac{E_2^*}{E_2} - (1 - \psi_1)\alpha VU_1\frac{E_1^*}{E_1}\\ & - (1 - \psi_2)\eta VU_2\frac{E_2^*}{E_2} - \frac{(1 - \psi_1)\alpha SU_1^*V^{*2}}{S^*V^*} - \frac{(1 - \psi_2)\eta SU_2^*V^{*2}}{S^*V^*} - \frac{\alpha r(1 - \theta)(S^* + (1 - \psi_1)V^*)U_1^*}{(\theta\mu + r)}\\ & - \frac{\eta a(1 - b)(S^* + (1 - \psi_2)V^*)U_2^*}{(b\mu + a)} - \frac{\alpha\theta\beta(S^* + (1 - \psi_1)V^*)E_1U_1^*}{\mu U_1} - \frac{\eta bp(S^* + (1 - \psi_2)V^*)E_2U_2^*}{\mu U_2}\\ & - \frac{\alpha r(S^* + (1 - \psi_1)V^*)Q_1U_1^*}{\mu U_1} - \frac{\eta a(S^* + (1 - \psi_2)V^*)Q_2U_2^*}{\mu U_2}, \end{aligned}$$

$$\begin{aligned} \dot{V}(x) = {} & \frac{-\mu}{S}(S - S^*)^2 + \mu V^*\left(3 - \frac{S^*}{S} - \frac{V}{V^*} - \frac{SV^*}{S^*V}\right) + k\alpha S^*U_1^*\left(3 - \frac{S^*}{S} - \frac{SU_1E_1^*}{S^*U_2^*E_1} - \frac{\theta\beta E_1}{k\mu U_1}\right)\\ & + s\eta S^*U_2^*\left(3 - \frac{S^*}{S} - \frac{SU_2E_2^*}{S^*U_2^*E_2} - \frac{bpE_2}{s\mu U_2}\right) + g\alpha S^*U_1^*\left(4 - \frac{S^*}{S} - \frac{SU_1E_1^*}{S^*U_1^*E_1} - \frac{rQ_1}{g\mu U_1} - \frac{r(1 - \theta)\beta E_1Q_1^*}{g\mu(\mu + r)U_1^*Q_1}\right)\\ & + h\eta S^*U_2^*\left(4 - \frac{S^*}{S} - \frac{SU_2E_2^*}{S^*U_2^*E_2} - \frac{aQ_2}{h\mu U_2} - \frac{a(1 - b)pE_2Q_2^*}{h\mu(\mu + a)U_2^*Q_2}\right) + k(1 - \psi_1)\alpha V^*U_1^*\left(4 - \frac{S^*}{S} - \frac{VU_1E_1^*}{V^*U_1^*E_1} - \frac{\theta\beta E_1}{k\mu Q_1} - \frac{SV^*}{S^*V}\right)\\ & + s(1 - \psi_2)\alpha V^*U_2^*\left(4 - \frac{S^*}{S} - \frac{VU_2E_2^*}{V^*U_2^*E_2} - \frac{bpE_2}{s\mu Q_2} - \frac{SV^*}{S^*V}\right) + g(1 - \psi_1)\alpha V^*U_1^*\left(5 - \frac{S^*}{S} - \frac{VU_1E_1^*}{V^*U_1^*E_1} - \frac{SV^*}{S^*V} - \frac{r(1 - \theta)\beta Q_1^*E_1}{g\mu(\mu + r)U_1^*Q_1} - \frac{rQ_1}{g\mu U_1}\right)\\ & + h(1 - \psi_2)\eta V^*U_2^*\left(5 - \frac{S^*}{S} - \frac{VU_2E_2^*}{V^*U_2^*E_2} - \frac{SV^*}{S^*V} - \frac{a(1 - b)pQ_2^*E_2}{h\mu(\mu + a)U_2^*Q_2} - \frac{aQ_2}{h\mu U_2}\right). \end{aligned} \tag{30}$$

By arithmetic-geometric means inequality, i.e., $n - (m_1 + m_2 + \cdots + m_n) \leq 0$, where $m_1.m_2 \ldots m_n = 1$ and $m_1, m_2, \ldots, m_n > 0$, it follows that $\dot{V} \leq 0$ with $V = 0$ if and only if $S = S^*$, $V = V^*$, $E_1 = E_1^*$, $E_2 = E_2^*$, $Q_1 = Q_1^*$, $Q_2 = Q_2^*$, $U_1 = U_1^*$, and $U_2 = U_2^*$. Hence, (W_1) is said to be GAS which follows LaSalle's Invariance Principle [12]. □

3.4. Sensitivity and Uncertainty Analysis. Figures 1 and 2 show the sensitivity and uncertainty analysis SA/UA of the obtained reproduction numbers for both variants with 2000 samples (up to 5 simulations for Figure 1 and a single simulation for Figure 2), getting a reliability indicator of 100%. From the SA in Figure 1(a), it is noticeable that the

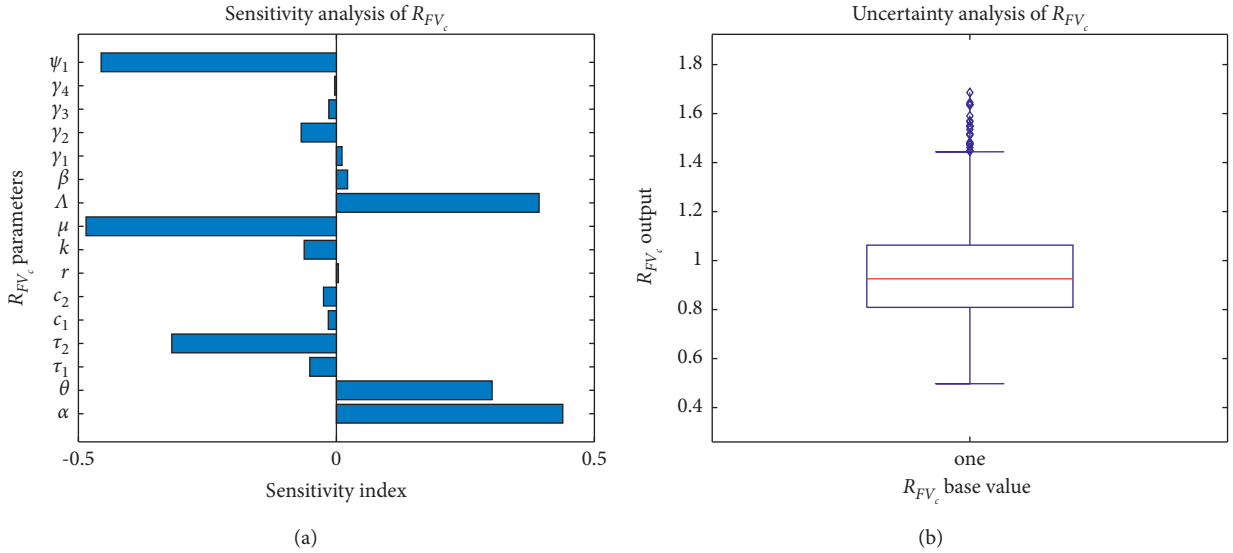

FIGURE 1: Global sensitivity and uncertainty analysis of variant 1. (a) Partial rank correlation coefficients (PRCC) for variant 1. (b) The box plot of variant 1.

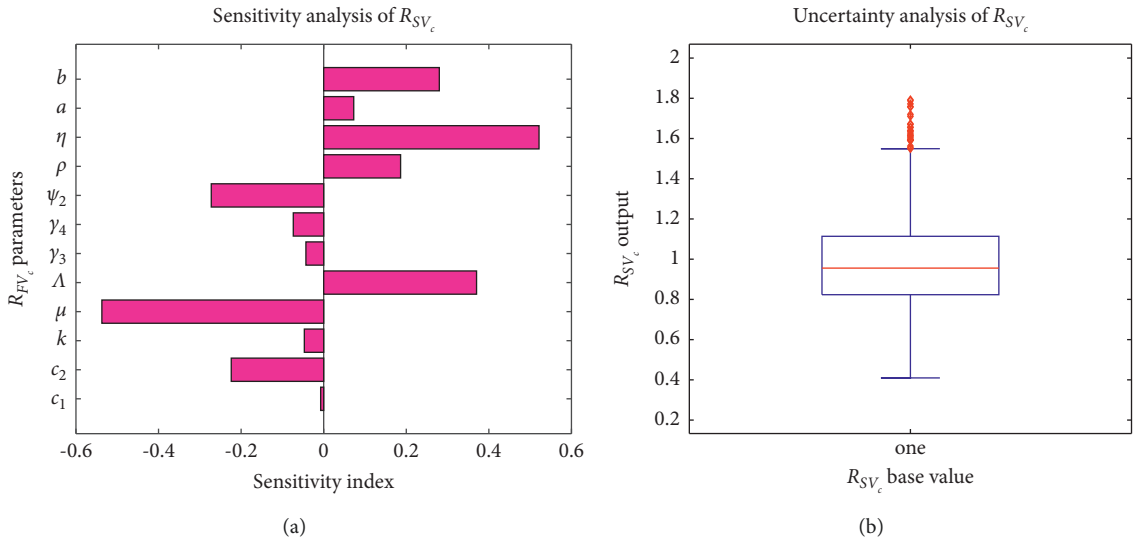

FIGURE 2: Global sensitivity and uncertainty analysis of variant 2. (a) Partial rank correlation coefficients (PRCC) for variant 2. (b) The box plot of variant 2.

parameters ψ_1, μ, and τ_1 contribute most to the disease reduction while the parameters Λ, θ, and α contribute to the spread of the disease. On the other hand, the UA in Figure 1(b) shows that the range of the R_{FV_c} is approximately [0.4 – 1.8], though most of the outputs are concentrated in low values ([0.4 – 1.1]). From the SA in Figure 2(a), it is noticeable that the parameters ψ_2, μ, and c_2 contribute most to the disease reduction while the parameters b, a, η, p, and Λ contribute to the spread of the disease. On the other hand, the UA in Figure 2(b) shows that the range ofR_{SV_c} is approximately [0.2 – 2], and most of the outputs are concentrated in low values ([0.2 – 1.1]).

4. Numerical Simulations and Discussion

This section presents numerical solutions of the proposed model and discussion of our findings. All simulations are done on MATLAB platform while parameter values used are in Table 1.

4.1. Investigation of Stability. Figure 3 shows the trajectories of the state variables in the proposed model when $R_c < 1$. Different initial values are used as shown in Figure 3. Although the number of individuals in the infected classes (i.e., exposed individuals, quarantined individuals, and undetected

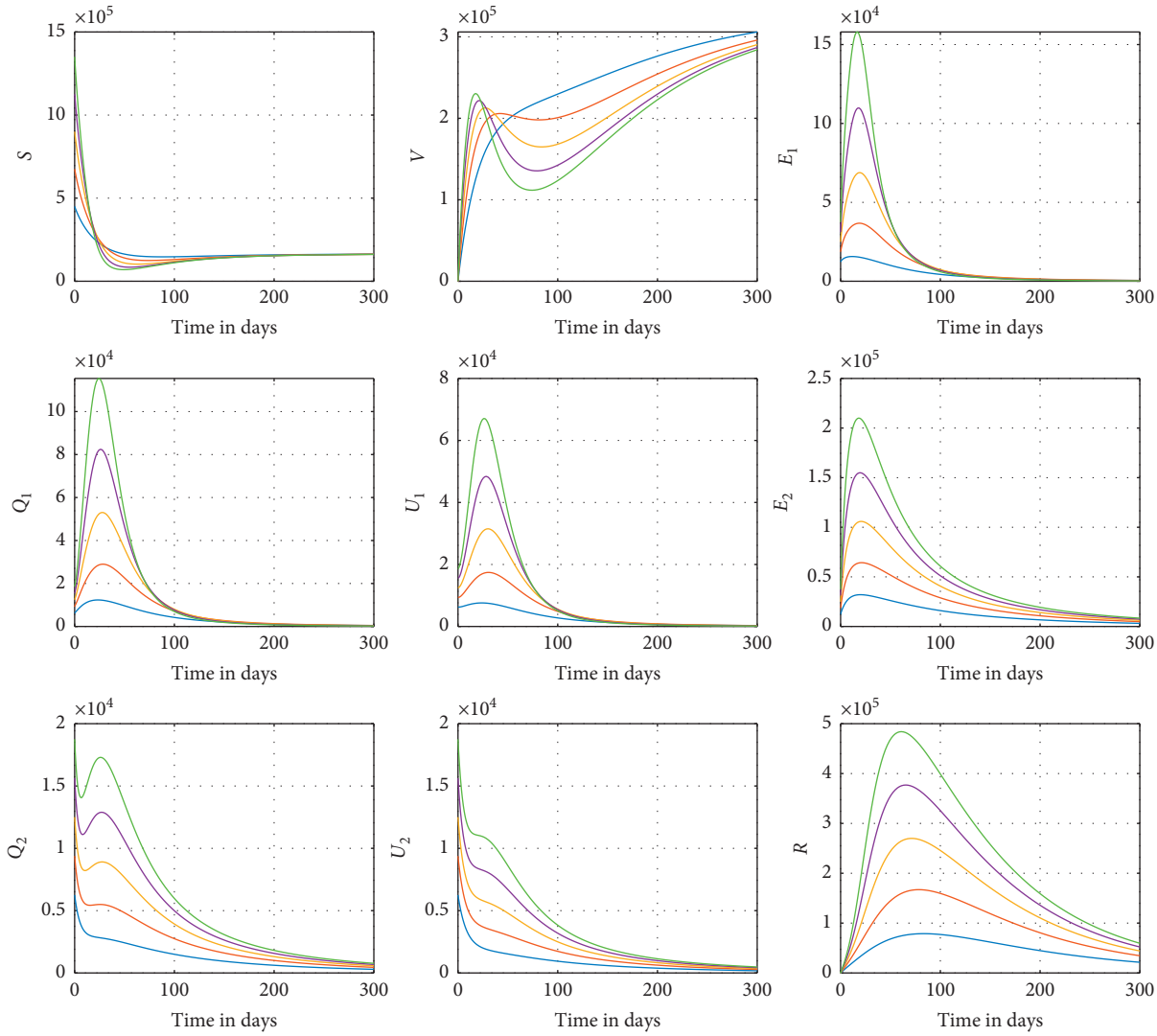

FIGURE 3: These graphs are obtained by numerically solving the proposed model using $\psi_1 = 0.7$ and $\psi_2 = 0.65$ and other parameter values as contained in Table 1. With this choice of parameter values, $R_c = 0.6742$, where S is the susceptible individuals, V is the vaccinated individuals, E_1 is the individuals exposed to variant 1, Q_1 is the quarantined individuals who are infected with variant 1, U_1 is the undetected individuals who are infected with variant 1, E_2 is the individuals exposed to variant 2, Q_2 is the quarantined individuals who are infected with variant 2, U_1 is the undetected individuals who are infected with variant 2, and R is the recovered individuals.

individuals) first increases, it later decreases and attains a disease-free state. This confirms the result in Theorem 1. In other words, the condition $R_0 < 1$ is sufficient for the disease control irrespective of the initial size of infection.

In Figure 4, the number of susceptible individuals decreases and reaches a stable equilibrium. The populations of the vaccinated individuals exhibit ups and downs until a stable equilibrium is reached. Infected classes (i.e., exposed individuals, quarantined individuals, and undetected individuals) approach the equilibrium position after early rises. It very well may be found in Figure 4 that the infectious population approaches the endemic point with $R_c > 1$. However, before approaching to endemic point, the infected individuals increase. Thus, after a certain percentage of the population has become vaccinated, infected, and recovered, the entire population will have certain level of indirect immunity. This is known as herd immunity.

4.2. Impact of Intervention Strategies. Figure 5 shows the impact of the new variant of SARS-CoV-2 in the presence of imperfect vaccine. $R_{FV_c} = 0.7899$ and $R_{SV_c} = 0.8287$ imply that the spread of variant 1 of SARS-CoV-2 is relatively under control than the spread of variant 2. Furthermore, Figure 5 shows that prevalence of variant 2 enhances the prevalence of variant 1. Thus, discovering a vaccine which is effective (to a good extent) for the prevention against variant 2 is necessary for the control of COVID-19.

Simulation in Figure 6 is done to investigate the impact of escape of quarantined infectious individuals from isolation centers. The parameters responsible for this are r and a. When $r = a = 0.01$, a good number of susceptible individuals become vaccinated leading to an increase in vaccinated population. This population later reduces as the susceptible population decreases (see subplot 1). It can also be seen from the subplots of 3–8 in

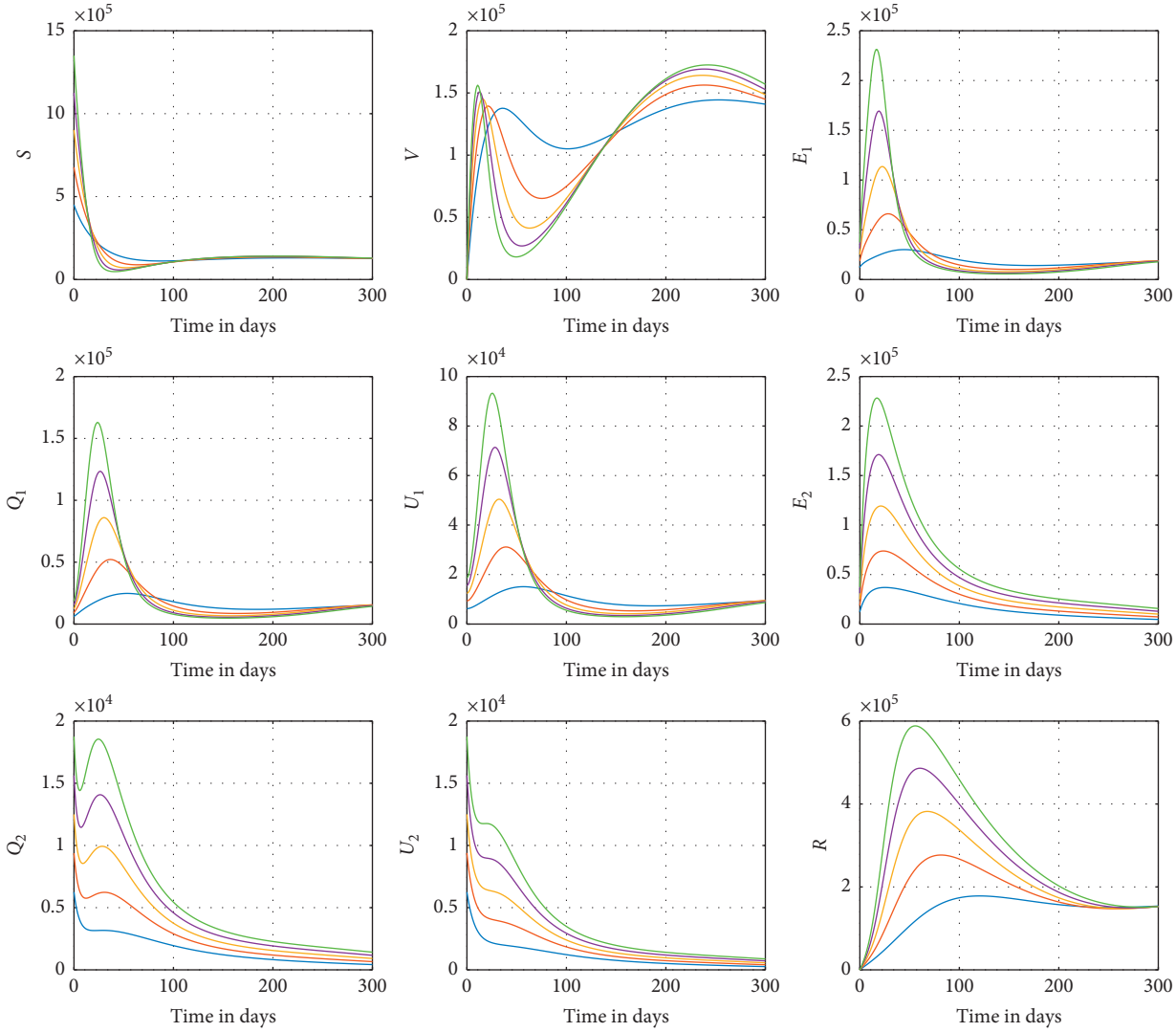

FIGURE 4: These graphs are obtained by numerically solving model 1 using parameter values as contained in Table 1. With this choice of parameter values $\psi_1 = \psi_2 = 0.1$, $\alpha = 0.6/N_0$, $\eta = 0.7/N_0$, and $R_c = 1.8883$, where S is the susceptible individuals, V is the vaccinated individuals, E_1 is the individuals exposed to variant 1, Q_1 is the quarantined individuals who are infected with variant 1, U_1 is the undetected individuals who are infected with variant 1, E_2 is the individuals exposed to variant 2, Q_2 is the quarantined individuals who are infected with variant 2, U_1 is the undetected individuals who are infected with variant 2, and R is the recovered individuals.

Figure 6 that, with increase in the rate at which individuals infected with variant 1 escape the isolation center, vaccination of susceptible individuals lowers the peak of the population infected with variant 2 while there is an increase in the population infected with variant 1. This is probably because individuals infected with variant 2 appear to be more careful with their lives and get vaccinated more than individuals infected with variant 1.

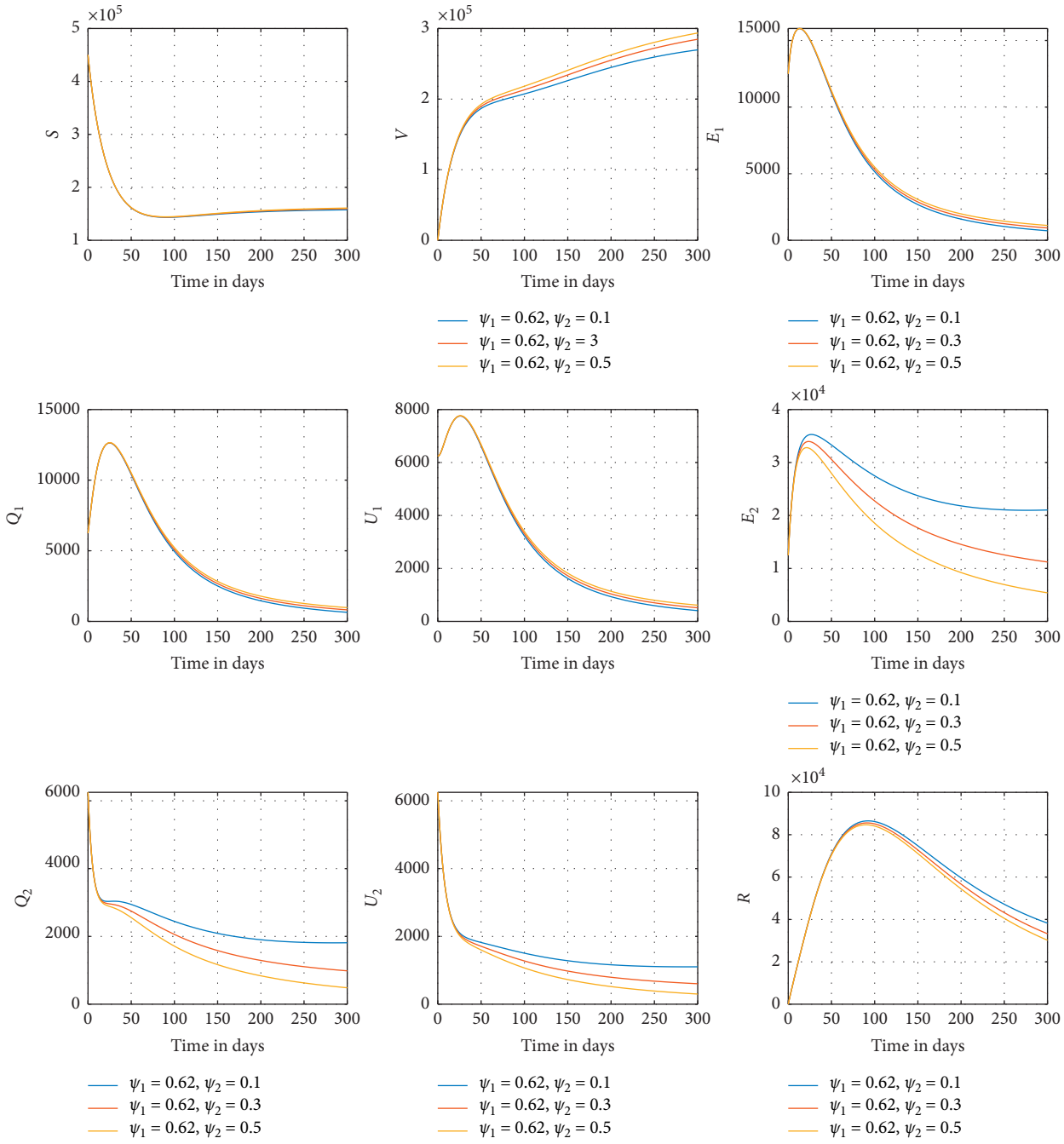

FIGURE 5: These graphs are obtained by numerically solving the model using $\psi_1 = 0.62$ and other parameter values as contained in Table 1. With this choice of parameter values, $R_{SV_c} = 0.8287$, where S is the susceptible individuals, V is the vaccinated individuals, E_1 is the individuals exposed to variant 1, Q_1 is the quarantined individuals who are infected with variant 1, U_1 is the undetected individuals who are infected with variant 1, E_2 is the individuals exposed to variant 2, Q_2 is the quarantined individuals who are infected with variant 2, U_1 is the undetected individuals who are infected with variant 2, and R is the recovered individuals.

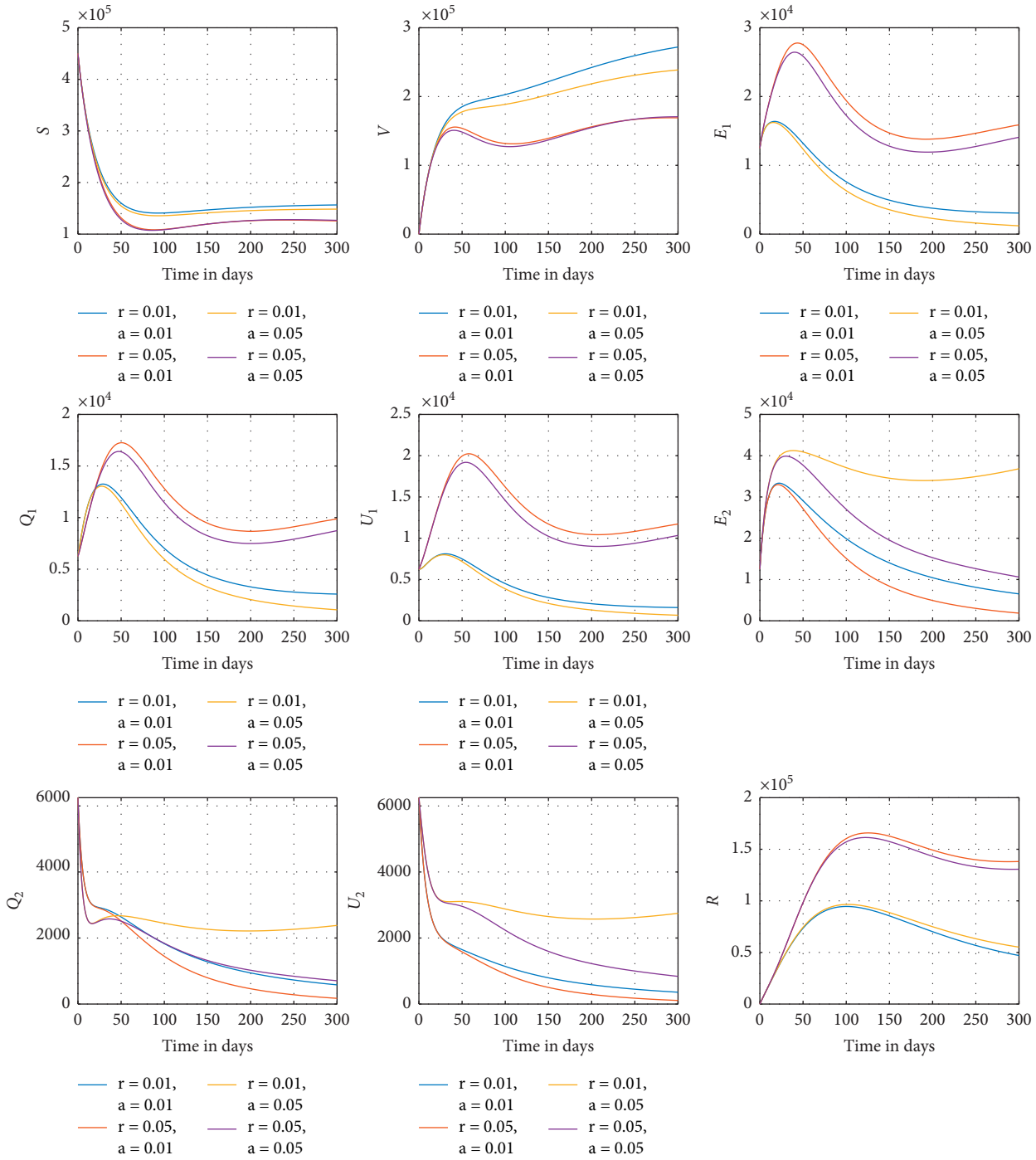

Figure 6: Investigation of the impact of escape of quarantined infectious individuals from isolation centers, where S is the susceptible individuals, V is the vaccinated individuals, E_1 is the individuals exposed to variant 1, Q_1 is the quarantined individuals who are infected with variant 1, U_1 is the undetected individuals who are infected with variant 1, E_2 is the individuals exposed to variant 2, Q_2 is the quarantined individuals who are infected with variant 2, U_1 is the undetected individuals who are infected with variant 2, and R is the recovered individuals.

5. Conclusion

We presented a COVID-19 model consisting of nine mutually exclusive compartments representing COVID-19 dynamics. The model considers a vaccinated population and a new variant of SARS-CoV-2 in which the vaccine is not perfect and the transmission rate of the new variant (second variant) of SARS-CoV-2 is higher than the transmission rate of the first variant. The model also considers the escape rate of quarantined infectious individuals. This study is necessary and important as it gives a clear understanding of the impact of the imperfect vaccine on the new variant (second variant).

Also, it gives an idea of the disease dynamics with the occurrence of a new variant of SARS-CoV-2. The control reproduction number, R_c, is obtained using the next-generation matrix method. The basic reproduction number R_0 is obtained from the control reproduction number, R_c, by setting the control measures to be zero, i.e., $\psi_1 = \psi_2 = \kappa = 0$. It is found that the control reproduction number, R_c, is given by the maximum of the two threshold quantities, R_{FV_c} and R_{SV_c}. It is shown that there are two possible equilibria of the model; one is a disease-free equilibrium that exists and is globally asymptotically stable if $R_c < 1$, and the other is endemic equilibrium which is shown to exist for $R_{SV_c} > 1$. Analytically, results reveal that the second variant (new variant) of SARS-CoV-2 dominates the first variant. Hence, the first variant of SARS-CoV-2 clears out of the population over time, even with the control reproduction number greater than one. Moreover, the first and second variant can only be cleared out of the population if R_{FV_c} and R_{SV_c} are less than one, i.e., $R_{FV_c}, R_{SV_c} < 1$. Further, the impact of the imperfect vaccine on the new variant is explored through numerical simulations. Numerical results reveal that individuals infected with the new variant (second variant) of SARS-CoV-2 who are vaccinated with an imperfect vaccine are under control but the prevalence of the second variant enhances the prevalence of the first variant. Numerical results also reveal that increase in the rate at which individuals infected with the first variant escape the isolation center gives rise to the population infected with the first variant and lowers the peak of the population infected with the second variant. This is probably because individuals infected with the second variant appear to be more careful with their lives and get vaccinated more than individuals infected with the first variant. As a result, current antiviral methods such as frequent hand washing, use of mask, physical separation, excellent ventilation, and avoiding crowded locations or enclosed settings continue to function against the first and second types by limiting viral transmission. This study can be extended by introducing fractional-order into the formulated model. In this case, the model will be given fractional differential equations. All these directions need more investigation, and therefore they shall be left for future works.

Data Availability

No data were generated or analyzed during the study.

Conflicts of Interest

The authors declare that they have no conflicts of interest or personal relationships that could have appeared to influence the work reported in this paper.

Acknowledgments

The authors would like to thank the Deanship of Scientific Research at Umm Al-Qura University for supporting this work by Grant Code: 22UQU4281337DSR01. Taif University Researchers Supporting Project number (TURSP-2020/31), Taif University, Taif, Saudi Arabia.

References

[1] Coronavirus, "Common Symptoms Preventive Measures and How to Diagnose it," 2020, http://www.caringlyyours.com/coronavirus.

[2] A. B. Gumel, C. C. McCluskey, and J. Watmough, "An sveir model for assessing potential impact of an imperfect anti-sars vaccine," *Mathematical Biosciences and Engineering*, vol. 3, no. 3, pp. 485–512, 2006.

[3] F. M. G. Magpantay, M. A. Riolo, M. D. d. e. Cellès, A. A. King, and P. Rohani, "Epidemiological consequences of imperfect vaccines for immunizing infections," *SIAM Journal on Applied Mathematics*, vol. 74, no. 6, pp. 1810–1830, 2014.

[4] X.-H. Zhang, A. Ali, M. A. Khan, M. Y. Alshahrani, T. Muhammad, and S. Islam, "Mathematical analysis of the tb model with treatment via caputo-type fractional derivative," *Discrete Dynamics in Nature and Society*, vol. 2021, pp. 1–15, 2021.

[5] T. Faniran, A. Ali, M. O. Adewole, B. Adebo, and O. O. Akanni, "Asymptotic behavior of tuberculosis between smokers and non-smokers," *Partial Differential Equations in Applied Mathematics*, vol. 5, Article ID 100244, 2022.

[6] M. A. Aba Oud, A. Ali, H. Alrabaiah, S. Ullah, M. A. Khan, and S. Islam, "A fractional order mathematical model for covid-19 dynamics with quarantine, isolation, and environmental viral load," *Advances in Difference Equations*, vol. 2021, no. 1, pp. 106–119, 2021.

[7] A. Ali, F. S. Alshammari, S. Islam, M. A. Khan, and S. Ullah, "Modeling and analysis of the dynamics of novel coronavirus (covid-19) with caputo fractional derivative," *Results in Physics*, vol. 20, Article ID 103669, 2021.

[8] Y. X. Li, M. G. Alshehri, E. A. Algehyne et al., "Fractional study of Huanglongbing model with singular and non- singular kernel," *Chaos, Solitons & Fractals*, vol. 148, Article ID 111037, 2021.

[9] A. Ali, S. Islam, M. R. Khan et al., "Dynamics of a fractional order zika virus model with mutant," *Alexandria Engineering Journal*, vol. 61, no. 6, pp. 4821–4836, 2022.

[10] J. K. K. Asamoah, Z. Jin, and G.-Q. Sun, "Non-seasonal and seasonal relapse model for q fever disease with comprehensive cost-effectiveness analysis," *Results in Physics*, vol. 22, Article ID 103889, 2021.

[11] N. Anggriani, M. Z. Ndii, R. Amelia, W. Suryaningrat, and M. A. A. Pratama, "A mathematical covid-19 model considering asymptomatic and symptomatic classes with waning immunity," *Alexandria Engineering Journal*, vol. 61, no. 1, pp. 113–124, 2022.

[12] A. Arsie and C. Ebenbauer, "Refining lasalle's invariance principle," in *Proceedings of the 2009 American Control Conference*, pp. 108–112, IEEE, St. Louis, MO, USA, June 2009.

[13] T. Chen, J. Rui, Q. Wang, Z. Zhao, J. A. Cui, and L. Yin, "A Mathematical Model for Simulating the Transmission of Wuhan Novel Coronavirus. Biorxiv 2020," Google Scholar, 2020, https://www.biorxiv.org/content/10.1101/2020.01.19.911669v1.

[14] T. S. Faniran, B. E A, P. R, and A. E O, "Global and sensitivity analyses of unconcerned covid-19 cases in Nigeria: a mathematical modeling approach," *WSEAS Transactions on Mathematics*, vol. 20, pp. 218–234, 20.

[15] J. K. K. Asamoah, E. Okyere, A. Abidemi et al., "Optimal control and comprehensive cost-effectiveness analysis for covid-19," *Results in Physics*, vol. 33, Article ID 105177, 2022.

[16] A. Ali, Q. Iqbal, J. K. K. Asamoah, and S. Islam, "Mathematical modeling for the transmission potential of zika virus with optimal control strategies," *The European Physical Journal Plus*, vol. 137, no. 1, pp. 146–230, 2022.

[17] A. Mohsen, H Fadhil Al-Husseiny, X. Zhou, and K. Hattaf, "Global stability of covid-19 model involving the quarantine strategy and media coverage effects," *AIMS public Health*, vol. 7, no. 3, pp. 587–605, 2020.

[18] K. Hattaf, N. Yousfi, and N. Yousfi, "Dynamics of sars-cov-2 infection model with two modes of transmission and immune response," *Mathematical Biosciences and Engineering*, vol. 17, no. 5, pp. 5326–5340, 2020.

[19] K. Hattaf, "A new generalized definition of fractional derivative with non-singular kernel," *Computation*, vol. 8, no. 2, p. 49, 2020.

[20] K. Hattaf, "Stability of fractional differential equations with new generalized hattaf fractional derivative," *Mathematical Problems in Engineering*, vol. 2021, Article ID 8608447, 7 pages, 2021.

[21] E. A. Iboi, C. N. Ngonghala, and A. B. Gumel, "Will an imperfect vaccine curtail the COVID-19 pandemic in the U.S.?" *Infectious Disease Modelling*, vol. 5, pp. 510–524, 2020.

[22] S. Olaniyi, O. S. Obabiyi, K. O. Okosun, A. T. Oladipo, and S. O. Adewale, "Mathematical modelling and optimal cost-effective control of covid-19 transmission dynamics," *The European Physical Journal Plus*, vol. 135, no. 11, p. 938, 2020.

[23] N. Nkamba and M. M. Martin Luther, "Modeling analysis of a seiqr epidemic model to asses the impact of undetected cases and containment measures of the covid-19 outbreak in Cameroon," *London Journal of Research in Science*, Natural and Formal, 2020.

[24] E. A. Iboi, O. Sharomi, C. N. Ngonghala, and A. B. Gumel, "Mathematical Modeling and Analysis of Covid-19 Pandemic in nigeria," 2020, https://www.medrxiv.org/content/10.1101/2020.05.22.20110387v2.

[25] G. Parra and A. J. Arenas, "Qualitative analysis of a mathematical model with presymptomatic individuals and two sars-cov-2 variants," *Computational and Applied Mathematics*, vol. 40, no. 6, pp. 199–225, 2021.

[26] H. M. Youssef, N. Alghamdi, M. A. Ezzat, A. A. El-Bary, and A. M. Shawky, "A proposed modified seiqr epidemic model to analyze the covid-19 spreading in Saudi Arabia," *Alexandria Engineering Journal*, vol. 61, no. 3, pp. 2456–2470, 2022.

[27] P. Healthwise, "A. Onwuzoo, Nigeria Can't Beat COVID-19 with Patients Fleeing Isolation Centres," 2020, https://healthwise.punchng.com/nigeria-cant-beat-covid-19-with-patients-fleeing-isolation-centres.

[28] S. O. Akindeinde, E. Okyere, A. O. Adewumi, R. S. Lebelo, O. O. Fabelurin, and S. E. Moore, "Caputo fractional-order seirp model for covid-19 pandemic," *Alexandria Engineering Journal*, vol. 61, no. 1, pp. 829–845, 2022.

[29] J. Ssebuliba, J. N. Nakakawa, A. Ssematimba, and J. Y. T. Mugisha, "Mathematical modelling of covid-19 transmission dynamics in a partially comorbid community," *Partial Differential Equations in Applied Mathematics*, vol. 5, Article ID 100212, 2022.

[30] S. Pal and I. Ghosh, "A mechanistic model for airborne and direct human-to-human transmission of covid-19: effect of mitigation strategies and immigration of infectious persons," *The European Physical Journal - Special Topics*, vol. 13, pp. 1–19, 2022.

[31] N. G. Davies, S. Abbott, R. C. Barnard et al., "Estimated transmissibility and impact of SARS-CoV-2 lineage B.1.1.7 in England," *Science*, vol. 372, no. 6538, Article ID eabg3055, 2021.

[32] F. Brauer, "Mathematical epidemiology: past, present, and future," *Infectious Disease Modelling*, vol. 2, no. 2, pp. 113–127, 2017.

[33] J. Amador, A. Gómez-Corral, D. Armesto, and A. Gómez-Corral, "Extreme values in sir epidemic models with two strains and cross-immunity," *Mathematical Biosciences and Engineering*, vol. 16, no. 4, pp. 1992–2022, 2019.

[34] M. O. Adewole, A. A. Onifade, F. A. Abdullah, F. Kasali, and A. I. M. Ismail, "Modeling the dynamics of covid-19 in Nigeria," *International Journal of Algorithms, Computing and Mathematics*, vol. 7, no. 3, pp. 67–25, 2021.

[35] N. M. Ferguson, D. Laydon, G. Nedjati-Gilani et al., "Impact of Non-pharmaceutical Interventions (Npis) to Reduce Covid-19 Mortality and Healthcare Demand," 2020, https://www.imperial.ac.uk/media/imperial-college/medicine/sph/ide/gida-fellowships/Imperial-College-COVID19-NPI-modelling-16-03-2020.pdf.

[36] Statista, "Statista," 2020, https://www.statista.com/statistics/580345/death-rate-in-nigeria.

[37] The World Bank, "The World Bank," 2020, https://data.worldbank.org/indicator/sp.dyn.cdrt.

[38] P. Van den Driessche and J. Watmough, "Reproduction numbers and sub-threshold endemic equilibria for compartmental models of disease transmission," *Mathematical Biosciences*, vol. 180, no. 1-2, pp. 29–48, 2002.

[39] H. Guo and M. Y. Li, "Global stability in a mathematical model of tuberculosis," *Canadian Applied Mathematics Quarterly*, vol. 4, no. 2, 2006.

[40] P. La Salle Joseph, *The Stability of Dynamical Systems*, Society for Industrial and Applied Mathematics, Philadelphia, PA, USA, 1976.